

Stress-based Classification of Electrocardiogram Signals Before and After Music Therapy using Heart Rate Variability and Machine Learning

Dhriti Rachepalli*

Saratoga High School, USA

*Corresponding Author

Dhriti Rachepalli, Saratoga High School, USA.

Submitted: 2023, Oct 05 ; Accepted: 2023, Oct 11: Published: 2023, Oct 26

Citation: Rachepalli, D. (2023). Stress-based Classification of Electrocardiogram Signals Before and After Music Therapy using Heart Rate Variability and Machine Learning. *Adv Mach Lear Art Inte*, 4(2), 66-76.

Abstract

The harmful impacts of excessive stress on people's health have been widely acknowledged, necessitating effective methods for its identification. Recognizing the importance of early stress detection and intervention, this research aims to contribute to the field of healthcare. To achieve this objective, this study classifies electrocardiogram (ECG) signals by assessing physio-psychological states, specifically stress and examines the role of music therapy in alleviating stress. ECG signals, recorded both before and after a music therapy session, were collected. Using signal processing techniques, essential features were extracted from these ECG signals, resulting in a more accurate identification of stress. Additionally, through experimentation and model evaluation, *k*-nearest Neighbors (KNN) and Classification and Regression Trees (CART) were determined to be the most effective models for this classification. Both models consistently yielded 90% accuracy. These identified extracted features and models are vital to effectively recognizing stress in ECG signals, offering valuable insights for future studies and clinical applications. This research contributes not only to the development of tools for stress detection but also to the understanding of the therapeutic impact of music.

Keywords: ECG, Classification, Stress, Music Therapy, Machine Learning, HRV, KNN, CART

1. Introduction

Cardiovascular health problems, conditions that affect the heart and blood vessels can lead to various disorders. These conditions can be caused by several different factors such as high blood pressure, a sedentary lifestyle, high cholesterol levels, smoking, and chronic stress [1,2]. Stress is a psychological and physiological response to challenging situations or demands. Stress often results in an elevated heart rate, increased blood pressure, and the release of stress hormones [3].

Prolonged and chronic stress can have detrimental effects on cardiovascular health, leading to the development and progression of heart diseases [4]. Increased sympathetic activity and reduced parasympathetic activity, can also lead to an imbalance in the autonomic nervous system. This can negatively impact heart rate variability and increase the risk of arrhythmias [5].

Electrocardiography is a non-invasive diagnostic technique used to record and analyze the electrical activity of the heart [6]. Electrocardiography involves placing electrodes on the skin's surface, which then detects the electrical signals generated by the heart's depolarization and repolarization processes [7]. These signals are recorded as waveforms that represent different phases of the cardiac cycle. An electrocardiogram (ECG) is the graphical representation of these signals. By interpreting ECGs, medical practitioners can assess the heart's function and detect irregularities such as arrhythmias, myocardial infarctions (heart attacks), and conduction abnormalities [8].

Clinically, ECGs are normally interpreted by an electrophysiology with a high level of expertise. ECG interpretation is time-consuming and dependent on individual interpretations [9]. The scarcity of medical experts, the complexity of ECG interpretations, and the similarities in the manifestations of heart abnormalities in ECG signals create challenges that can be addressed through machine learning [10]. Early detection through machine learning used to require long-term monitoring (more than 24 hours) of the heart. However, there have been rapid improvements in devices, data acquisition, and machine-learning techniques [11].

Heart Rate Variability (HRV) is a critical physiological measure derived from ECG signals that offer valuable insights into the autonomic nervous system's activity, specifically the balance between sympathetic and parasympathetic branches [12]. HRV quantifies the variation in time intervals between successive heartbeats, known as RR intervals, and reflects the dynamic nature of heart rate modulation [13]. Stress and anxiety often lead to decreased HRV, indicating a reduced ability to regulate stress and a shift towards a more sympathetic-dominant state. On the other hand, relaxed states and positive emotions are associated with higher HRV, reflecting enhanced vagal tone and greater parasympathetic modulation [14].

To detect and analyze stress through ECG signals, several machine-learning techniques have been utilized in numerous studies. These techniques include K-Nearest Neighbor (KNN), Linear Discriminant Analysis, Linear Regression, Naive Bayes, Random Forest, AdaBoost, and, most commonly, Support Vector Machine (SVM) [15-20]. The accuracy of the data is also commonly improved by applying 10-fold cross-validation [20].

In the study conducted by Garg et al., the main objective was to detect stress. The study included KNN, Linear Discriminant Analysis, Random Forest, AdaBoost, and SVM. The Random Forest model outperformed other models with F1 scores of 83.34 and 65.73 for binary classification and three-class classification [17]. Similarly, the study conducted by Ahuja and Banga aimed to analyze stress in college students. The study compared Linear Regression, Naive Bayes, Random Forest, and SVM and found that SVM produced the highest accuracy (85.71 percent) [20].

The field of ECG-based stress detection and music's influence on stress remains relatively underexplored. There are only a few studies that directly investigate the interplay between ECG signals, music, and stress responses. Therefore, further research in this domain is essential to establish robust and reliable methods for stress assessment using ECG and to better understand how music can modulate stress-related physiological responses.

The primary objective of this research endeavor is to develop a sophisticated model capable of accurately distinguishing between states of stress and relaxation in individuals. As music has long been associated with emotions and well-being, this investigation seeks to unravel the potential therapeutic impact of classical compositions on the human cardiovascular system. By harnessing the power of data-driven analysis and cutting-edge algorithms, the model will discern intricate ECG features, capturing the subtle shifts in heart rate variability and related parameters that may emerge in response to the calming influence of classical tunes. The model can revolutionize stress management and wellness practices and can pave the way for interventions tailored to each individual's unique physiological response.

2. Materials and Methods

2.1 Dataset Description

The data used in this paper is from the Combined measurement of ECG, Breathing, and Seismocardiograms DataBase (CEBSDB) from the Physionet database [21,22]. CEBSDB contains ECG signals for 20 presumed healthy volunteers. The subjects are all Caucasian with ages ranging from 19 to 30 years old. 8 subjects are female while the remaining 12 subjects are male, and all but one subject are non-smokers. At the time of the experiment, 8 subjects had recent coffee intake while 12 subjects did not and 8 subjects had a sedentary lifestyle while 12 subjects had a healthy lifestyle. Using a Biopac MP36 data acquisition system, channels 1 and 2 of the system measured conventional ECG while the subjects stayed still in a supine position on a comfortable conventional single bed. The subjects remained awake as the sensors were attached and the basal state was recorded for 5 minutes (records b001 to b020 in the dataset). The subjects listened to classical music for approximately 50 minutes and after the music ended, their ECG signals were once again measured and recorded for 5 minutes (records p001 to p020 in the dataset).

2.2 Pre-Processing

The ECG signals were initially sampled at a rate of 5000 Hz. The Nyquist Theorem states that the signal must be sampled at a rate more than twice the maximum frequency of the obtained signal [23]. It's written as $f_{\text{sample}} \geq 2f_{\text{max}}$ (1)

Since ECG signals normally have a frequency range of [0, 150] Hz, the data was down-sampled to a sampling rate of $2 \times 150 = 300$ Hz.

The `scipy.signal.resample` function from the Scipy library was used to downsample the ECG data [24]. The `resample` function utilized the Fast Fourier Transform (FFT) method for this purpose. FFT is an efficient algorithm for computing the Discrete Fourier Transform (DFT) of a sequence of numbers. Compared to standard DFT calculation, FFT is much less computationally complex, making it ideal for signal processing. DFT is a technique that transforms a discrete sequence of numbers from the time domain into the frequency domain. DFT is defined by the formula

$$X_k = \sum_{n=0}^{N-1} x_n e^{-i \frac{2\pi}{N} kn}, \quad k = 0, \dots, N-1 \quad (2)$$

Where x_n is the n -th data point in the original time domain signal, N is the number of data points in x_n , $e^{j2\pi/N}$ is a complex number with a magnitude of 1 and an argument (angle) of $2\pi/N$ radians, and k is the frequency index ranging from 0 to $N-1$ [25].

To eliminate redundant data, minimize errors, and make the information more machine-readable, the data was then normalized from 0-1 following the equation $X' = \frac{X - X_{\min}}{X_{\max} - X_{\min}}$ (3)

where X is each data point in the ECG signal, X_{\min} is the minimum value of the ECG signal, and X_{\max} is the maximum value of the ECG signal.

Utilizing the `scipy.signal.butter` function from the Scipy library, the normalized data was passed through a Butterworth bandpass filter of 0.05 to 149 Hz with an order of 2 [26]. A Butterworth filter is designed to have a maximally flat frequency response within its passband, resulting in minimal distortion of the filtered signal.

Its typical transform function is given as: $H_a(j\Omega) = \frac{1}{\sqrt{1 + \left(\frac{\Omega}{\Omega_c}\right)^{2N}}}$ (4)

where N is the order of the filter, j is the imaginary unit, Ω is the angular frequency, and Ω_c is the cutoff frequency [27].

In this study, the Butterworth filter was configured to function as a bandpass filter. A bandpass filter is characterized by two cutoff frequencies, the lower cutoff frequency and the higher cutoff frequency [28]. Frequencies below the lower cutoff and above the higher cutoff are removed.

The signals were then divided into two classes. Label 0 represents the signals measured before classical music was played and label 1 represents the signals measured after classical music was played. Records b001 to b020 were labeled 0 and records p001 to p020 were labeled 1.

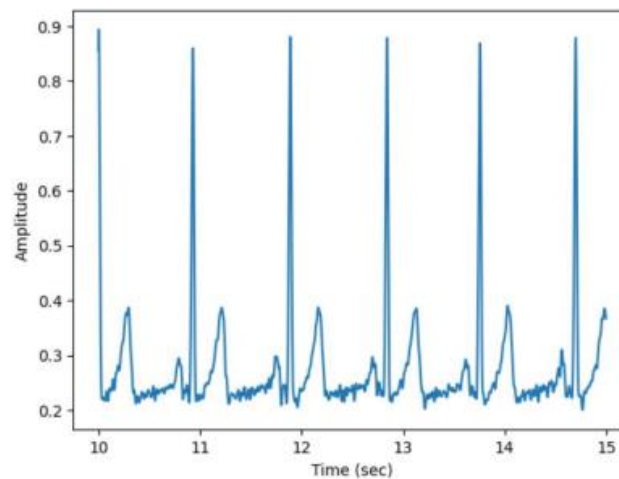


Figure 1: 5 seconds of the Processed ECG Data of Subject 1 Before Listening to Music (label 0)

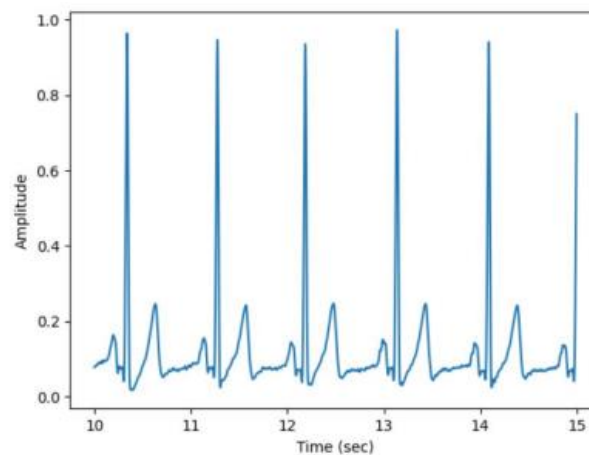


Figure 2: 5 seconds of the Processed ECG Data of Subject 1 After Listening to Music (label 1)

2.3 Feature Extraction

To clearly identify any changes in the stress of the subjects after listening to classical music, 18 relevant features of the subjects' ECG signals were extracted. These features are listed in Table 1.

Mean	Arithmetic average of all data
Standard Deviation (Std)	Spread of data points around the mean
Minimum	Lowest electrical activity observed
Maximum	Highest electrical activity observed
Mean of RR	Average duration between R-peaks
Std of RR	Variability in the time between R-peaks
IQR of RR	Range between the 25th and 75th percentiles
Sq. Root Diff. of RR	Variation in RR intervals
Minimum of RR	Shortest duration between two R-peaks
Maximum of RR	Longest duration between two R-peaks
QRS Duration	Time for ventricles to depolarize and contract
PR Duration	Start of P-wave to start of QRS complex
ST Duration	Period between QRS complex and T wave
QT Duration	Start of QRS complex to end of T-wave
HRV_LF	Low-frequency heart rate variability
HRV_HF	High-frequency heart rate variability
HRV_LFHF	Ratio of HRV_LF to HRV_HF
Heartrate	Calculated using RR intervals

Table 1: Description of All Extracted Features

To get the heart rate (see Fig. 3), QRS duration, PR duration, ST duration, and QT duration, Neurokit's ECG process () function was necessary [29]. When this function was called, the ecg delineate () function was also automatically invoked. The ECG delineate () function specifies a peak's location, amplitude, duration, and any other relevant attributes in an ECG. This allowed for the identification of QRS complexes (R-peaks), P-peaks, T-peaks, and other relevant peaks.

This function utilized Discrete Wavelength Transform (DWT) for the delineation. DWT decomposed the signal into multiple scales, each representing different frequency components. Peaks in the signal were highlighted as significant coefficients at specific scales, allowing for enhanced feature detection. Peak detection algorithms were then applied to these DWT coefficients to identify and delineate peaks. DWT can be written as

$$d_{j,k} = \int_{-\infty}^{\infty} s(t) \frac{1}{\sqrt{2^j}} \psi \left(\frac{t - k2^j}{2^j} \right) dt \quad (5)$$

where ψ is the mother wavelength and $d_{j,k}$ are known as wavelet coefficients at level j and location k [30].

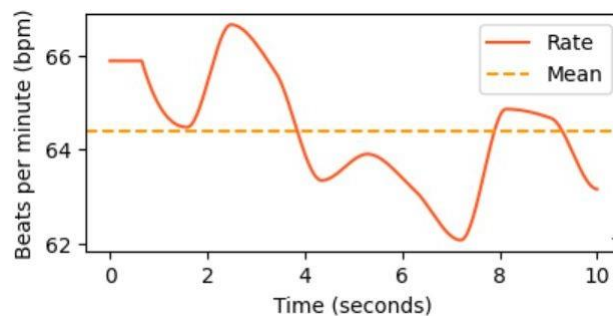


Figure 3: A visual of Subject 1's heart rate

Three of the features in Table 1 are considered HRV features: HRV_LF, HRV_HF, and HRV_LFHF is the measure of the variation in time between successive heartbeats. It quantifies the fluctuations in the time intervals between successive R-wave peaks in an ECG signal. In this study, only HRV frequency-domain features were obtained through the Neurokit library [31]. To acquire these features, the signal was segmented and windowed and FFT was once again applied. Then, the power spectrum of each segment was calculated by squaring the FFT result. The equation is

$$Pxx(k) = \frac{1}{N} |X(K)|^2, k = 0, 1, 2, \dots, N - 1 \quad (6)$$

where $Pxx(k)$ represent the Power Spectral Density (PSD) at frequency bin k , N is the number of data points in your signal, and $X(k)$ is the DFT formula defined earlier in the equation 2 [32]. The PSD revealed the power associated with each frequency component and was used to calculate HRV_LF, HRV_HF, and HRV_LFHF.

2.4. Feature Visualization

In order to ensure that the extracted features used were important and necessary for the machine learning models' improved accuracy, feature visualization was necessary.

The correlation matrix was used to determine the correlation coefficient between two features and evaluate their linear dependency. The correlation matrix utilized in this study is from the Pandas library and is based on Pearson's correlation coefficient [33]. For a correlation

between variables x and y , the formula is
$$r = \frac{\sum_{i=1}^n (x_i - \bar{x})(y_i - \bar{y})}{\sqrt{\sum_{i=1}^n (x_i - \bar{x})^2 \sum_{i=1}^n (y_i - \bar{y})^2}} \quad (7)$$

where n is the number of data points and x_i and y_i represent individual data points in x and y [34].

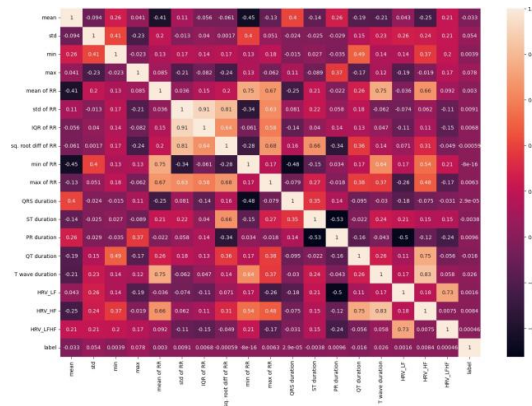


Figure 4: Correlation matrix of all features

The closer the correlation coefficient is to -1 or 1, the stronger the relationship is. Features with high correlation are more linearly dependent on each other and will have similar information [35]. In the correlation matrix, the IQR of RR feature and the std of RR feature had a high correlation coefficient: 0.91. To reduce redundancy and improve the stability of the model, the std of RR feature was removed as well.

When the correlation coefficient between two features is low (closer to 0), it could indicate that the feature does not contribute substantial information [36]. The QRS duration feature had weak relationships with all the other features. Many of its correlation coefficients were close to 0, with its highest only being 0.40. Due to this, the QRS duration feature was removed as well.

The features were also visualized as boxplots through the Pandas library [37]. Each graph contained two boxplots, one for each class (before and after listening to music).

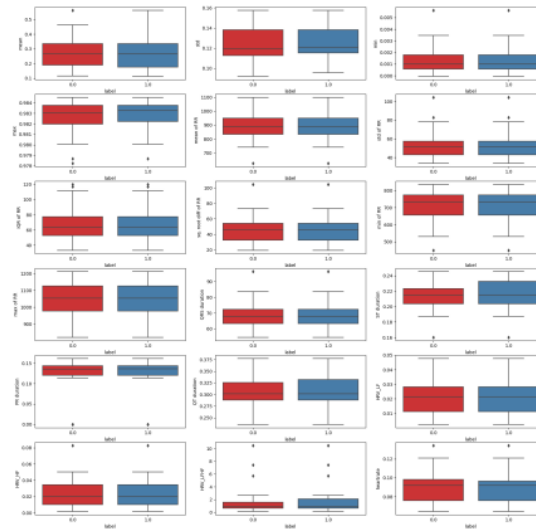


Figure 5: Boxplots of all features for signals obtained before music (label 0) and after music (label 1)

The boxplots revealed whether there were significant differences between the extracted features from each class. There were 7 features that displayed any visible differences: mean, std, max, PR duration, QT duration, HRV_LFHF, and heartrate. Another feature matrix was created containing only these 7 features.

2.4 Principal Component Analysis (PCA)

PCA reduces the complexity and dimensionality of the data, often improving the performance of machine learning models. PCA retains the most significant patterns and discards less important features, making it easier to work with large datasets.

PCA consists of data standardization, the covariance matrix, and eigenvalue decomposition. The formula to find the largest eigenvalue is

$$\max_v v^T \tilde{X}^T \tilde{X} v \quad s.t. \quad \|v\| = 1 \quad (8)$$

where v is an eigenvector, X is a matrix of data, v^T is the transpose of v , and X^T is the transpose of X [38].

The number of components for PCA was chosen using the graph of the cumulative explained variance. In order to explain around 99% of the variance, this study used four components.

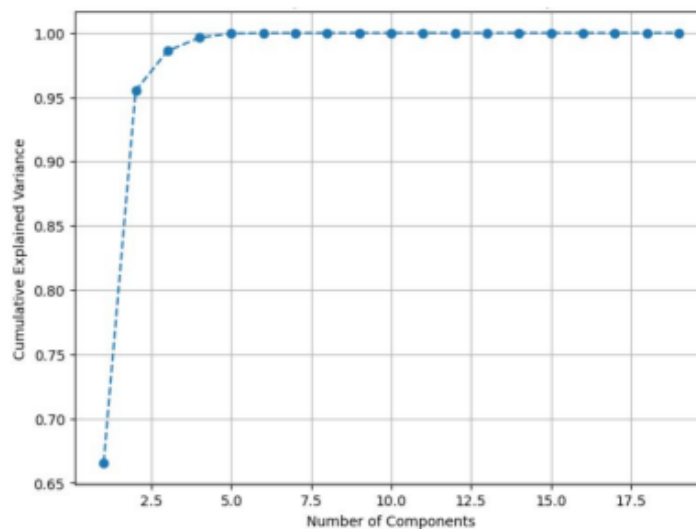


Figure 6: Cumulative Explained Variance for PCA Components

As this research didn't have a large dataset, it was necessary to compare the results of using PCA with the results of not using PCA.

2.5 Machine Learning Models

This study compared the results of 6 machine learning models: Linear Regression (LR), K-Nearest Neighbors (KNN), Classification and Regression Trees (CART), Gaussian Naïve Bayes (NB), Support Vector Machine (SVM), XGBoost, and Linear Discriminant Analysis (LDA) [39–45].

Model	Description
LR	Fits a linear equation to observed data
KNN	Classifies based on the majority class of K nearest neighbors
CART	Recursively splits data into subsets to create tree-like structure
NB	Bayes' theorem; uses conditional probabilities for classification
SVM	Finds hyperplane that maximizes separation between classes
LDA	Reduces data dimensions while maximizing class separation

TABLE 2: Models

2.6 Training and Testing Sets

The purpose of this study was to classify ECG signals as either before music therapy or after music therapy. However, the differences between the ECG signals before and after music therapy were very minute. As these signals were highly correlated, it was important to ensure both signals from each subject stayed together in either the training or testing set. If both signals did not stay together, it could have led to overfitting as the models learned to memorize the training data [46]. It could've also resulted in data leakage where information from the testing set influenced the training of the model [47]. The models would've then learned to recognize patterns specific to the subject, rather than general patterns. In the case of both overfitting and data leakage, the models would've performed well on the testing data but poorly on unseen data. In this study, 80% of the subjects were placed in the training set and the remaining 20% were placed in the testing set. Both ECG signals of each subject stayed together during the splitting. Thus, there were 32 samples in the training set and 8 in the testing set.

3. Results

3.1 Cross-validation

Cross-validation is a widely used technique to assess the performance of a machine learning model. Compared to a single train-test split, cross-validation is more robust. If a model performs well on the training data but poorly on the testing data in multiple cross-validation iterations (folds), it can indicate overfitting. Furthermore, cross-validation uses the data for both training and testing and increases efficiency, which is helpful for small datasets. As cross-validation finds the average of multiple folds, the variability in the model's performance is reduced.

The form of cross-validation used in this study was the k-fold cross-validation. This form splits the data into k equal-sized subsets. The model was then trained and tested k times where for each iteration, one subset was used as the test set, and the remaining k-1 subsets were used as the training set. For each iteration, performance metrics (such as accuracy and precision) were calculated. The general equation is $Performance\ Estimate = \frac{1}{n} \sum_{i=1}^n Loss(y_i, \hat{f}_{-k}(x_i))$ (9)

where n is the number of data points, y_i is the true target value for the i-th data point, and $\hat{f}_{-k}(x_i)$ is the predicted value for the i-th data point obtained using the model trained on all but the kth subset [48]. This study used 4 folds to produce the best results.

3.2 Comparison of Results

Model	Accuracy	Standard Deviation
For All Features		
LR	0.2500	0.0883
KNN	0.4063	0.1036
CART	0.2188	0.0541
NB	0.3125	0.0625

SVM	0.3125	0.0625
LDA	0.1875	0.1398
For PCA		
LR	0.2991	0.0462
KNN	0.294643	0.0949
CART	0.1964	0.0536
NB	0.2679	0.0902
SVM	0.200893	0.0684
LDA	0.2991	0.0462
For Specific Features		
LR	0.7679	0.1763
KNN	0.9688	0.0541
CART	0.9330	0.0673
NB	0.8000	0.1247
SVM	0.8705	0.0887
LDA	0.7679	0.1763

Table 3: Training Accuracies

3.3 Best Results

When the models were trained on the seven specifically chosen features (mean, std, max, PR duration, QT duration, HRV_LFHF, heart rate), the accuracies were the highest

Model	Accuracy	Precision	Recall	f1
Training Set				
LR	0.7679	0.7667	0.8125	0.7817
KNN	0.9688	0.9500	1.0000	0.9722
CART	0.9330	0.9500	0.9167	0.9222
NB	0.8000	0.8700	0.8000	0.7814
SVM	0.8705	0.8875	0.8750	0.8740
LDA	0.7679	0.7667	0.8125	0.7817
Testing Set				
LR	0.50	0.50	1.00	0.67
KNN	0.90	0.83	1.00	0.91
CART	0.90	0.83	1.00	0.91
NB	0.60	0.56	1.00	0.71
SVM	0.80	0.71	1.00	0.83
LDA	0.50	0.50	0.40	0.44

Table 4: Results for Specific Features

The table above contains the precision, recall, and f1 scores of different models trained on the seven features.

Precision is a performance metric that measures the accuracy of positive predictions made by the model. The equation is given as

$$Precision = \frac{TP}{TP + FP} \quad (10)$$

where *TP* is the true positives and *FP* is the false positives. Recall is the ability of a model to correctly identify all instances of a class in a dataset. Recall is calculated by the formula

$$Precision = \frac{TP}{TP + FN} \quad (11)$$

where FN is the false negatives. The F1 score combines both precision and recall into a single metric using the equation

$$F1 = \frac{Precision * Recall}{Precision + Recall} \quad (12)$$

The F1 score is another measure of accuracy [49].

4. Discussion

This study's method involved several key steps in the data processing and analysis pipeline. Firstly, pre-processing was performed on the raw data, which included normalization, down sampling using Fast Fourier Transform (FFT), and band-pass filtering to retain frequency components between 0.05 and 149 Hz. Next, during feature extraction, peaks in the signal were identified using Discrete Wavelet Transform (DWT), and Heart Rate Variability (HRV) features were computed using Power Spectral Density (PSD) analysis. For feature selection and visualization, boxplots were employed to identify seven features that exhibited significant differences between the before music therapy and after music therapy groups. To reduce dimensionality and aid in visualization, we applied Principal Component Analysis (PCA) and determined that using four components effectively captured the data's variance. The models' results obtained with PCA, without PCA, and without PCA using the seven specific features were compared to determine the best results.

This method was chosen based on insights from existing literature, which highlighted the most commonly employed models and techniques for ECG signal analysis. To ensure the robustness of this study's analysis, widely recognized and established methodologies were used to ensure the robustness of our analysis. Standard techniques such as Principal Component Analysis (PCA) and cross-validation were employed to optimize model performance, enhancing the reliability of this study's findings. Furthermore, widely accepted evaluation metrics, such as precision and the F1 score, were used to assess the functionality and effectiveness of the selected models, providing a comprehensive and rigorous approach to this research.

The results of this study revealed that K-Nearest Neighbors (KNN) and Classification and Regression Trees (CART), both rooted in decision tree algorithms, yielded the best predictive testing accuracies for the classification of ECG signals before and after music therapy based on stress. Although KNN performed better than CART on the testing set with an accuracy of 96.9%, both models achieved an accuracy of 90% on the testing set. This outcome underscores the potential of these decision tree-based models and emphasizes the effectiveness of the seven specific features this study identified. These findings suggest that KNN and CART models, in combination with the identified features, can be leveraged to produce more accurate stress detection results in various contexts.

However, there are limitations in this study. One of the most prominent constraints is the size of the dataset, which contains only 40 samples and is notably small. This limitation restricts the amount of data available for model training and evaluation, potentially impacting the generalization of the findings. Especially since the data from both of the classes were highly correlated, there could have been data leakage, resulting in inflated accuracies. External validation, which is the assessment of our model's performance on entirely new, unseen data, also remains an area of further exploration. Moreover, the diversity of subjects within the dataset is limited, which may affect the applicability of this study's results to broader populations. Lastly, despite the use of cross-validation to mitigate overfitting, the possibility of overfitting persists, particularly given the dataset's size and complexity. These limitations provide insights into areas where future research and data collection efforts can enhance the robustness and applicability of these findings.

There are several promising areas of improvement for future works and research. First and foremost, expanding the dataset's size is imperative, allowing for a more comprehensive analysis and strengthening the generalizability of this study's findings. Increasing the diversity of the dataset by including a broader range of subjects and scenarios would also enhance the model's adaptability to various real-world contexts. Another important improvement is the subdivision of stress into different levels or categories, providing a more nuanced understanding of stress responses. Dividing stress into levels allow for a greater understanding of an individual's stress response, which can be especially useful in healthcare and psychology. The levels would provide a more comprehensive picture of how stress affects individuals and the impact music therapy has on people with different levels of initial stress. Moreover, advanced machine learning techniques, such as deep learning and transfer learning, hold potential for improving predictive accuracy. These techniques identify intricate patterns within physiological signals which may be challenging to extract using traditional methods. Such approaches could capture nuanced variations in stress responses, leading to more precise predictions. Finally, the development of a real-time monitoring system would allow for continuous assessment, increasing the size of the dataset. This system, valuable for both research and practical applications, would result in greater accuracy.

5. Conclusion

This study demonstrates a robust methodology for classifying ECG signals based on stress with high accuracy, while also determining

pivotal features necessary for this precise classification. The ability to reliably identify physio-psychological states, particularly stress, is crucial for healthcare practitioners, therapists, and researchers. It deepens comprehension of stress-related health conditions, facilitating early intervention and personalized treatment plans. Additionally, these findings have the potential to make a substantial impact on the field of music therapy. By demonstrating the effectiveness of stress identification models, this study provides the foundation for quantifying the influence of music therapy on stress reduction. This, in turn, can guide the development of music therapy precisely tailored to individuals' stress levels. Ultimately, this research contributes to a future where music therapy can be optimized to effectively enhance the well-being of a wide range of individuals.

References

1. Benjamin, E. J., Muntner, P., Alonso, A., Bittencourt, M. S., Callaway, C. W., Carson, A. P., ... & American Heart Association Council on Epidemiology and Prevention Statistics Committee and Stroke Statistics Subcommittee. (2019). Heart disease and stroke statistics—2019 update: a report from the American Heart Association. *Circulation*, 139(10), e56-e528.
2. Gaziano, T. A., Bitton, A., Anand, S., Abrahams-Gessel, S., & Murphy, A. (2010). Growing epidemic of coronary heart disease in low-and middle-income countries. *Current problems in cardiology*, 35(2), 72-115.
3. Chrousos, G. P. (2009). Stress and disorders of the stress system. *Nature reviews endocrinology*, 5(7), 374-381.
4. Rozanski, A., Blumenthal, J. A., & Kaplan, J. (1999). Impact of psychological factors on the pathogenesis of cardiovascular disease and implications for therapy. *Circulation*, 99(16), 2192-2217.
5. Thayer, J. F., Hansen, A. L., Saus-Rose, E., & Johnsen, B. H. (2009). Heart rate variability, prefrontal neural function, and cognitive performance: the neurovisceral integration perspective on self-regulation, adaptation, and health. *Annals of behavioral medicine*, 37(2), 141-153.
6. Birnbaum, Y., Nikus, K., Kligfield, P., Fiol, M., Barrabés, J. A., Sionis, A., ... & de Luna, A. B. (2014). The role of the ECG in diagnosis, risk estimation, and catheterization laboratory activation in patients with acute coronary syndromes: A consensus document. *Annals of Noninvasive Electrocardiology*, 19(5), 412-425.
7. Kligfield, P., Gettes, L. S., Bailey, J. J., Childers, R., Deal, B. J., Hancock, E. W., ... & Wagner, G. S. (2007). Recommendations for the standardization and interpretation of the electrocardiogram: part I: the electrocardiogram and its technology: a scientific statement from the American Heart Association Electrocardiography and Arrhythmias Committee, Council on Clinical Cardiology; the American College of Cardiology Foundation; and the Heart Rhythm Society endorsed by the International Society for Computerized Electrocardiology. *Circulation*, 115(10), 1306-1324.
8. Tso, C., Currie, G. M., Gilmore, D., & Kiat, H. (2015). Electrocardiography: A technologist's guide to interpretation. *Journal of nuclear medicine technology*, 43(4), 247-252.
9. Mincholé, A., Camps, J., Lyon, A., & Rodríguez, B. (2019). Machine learning in the electrocardiogram. *Journal of electrocardiology*, 57, S61-S64.
10. Ayano, Y. M., Schwenker, F., Dufera, B. D., & Debelee, T. G. (2022). Interpretable machine learning techniques in ECG-based heart disease classification: a systematic review. *Diagnostics*, 13(1), 111.
11. Alfaras, M., Soriano, M. C., & Ortín, S. (2019). A fast machine learning model for ECG-based heartbeat classification and arrhythmia detection. *Frontiers in Physics*, 103.
12. Vanderlei, L. C. M., Silva, R. A., Pastre, C. M., Azevedo, F. M. D., & Godoy, M. F. (2008). Comparison of the Polar S810i monitor and the ECG for the analysis of heart rate variability in the time and frequency domains. *Brazilian Journal of Medical and Biological Research*, 41, 854-859.
13. Schäfer, A., & Vagedes, J. (2013). How accurate is pulse rate variability as an estimate of heart rate variability?: A review on studies comparing photoplethysmographic technology with an electrocardiogram. *International journal of cardiology*, 166(1), 15-29.
14. Castaldo, R., Melillo, P., Bracale, U., Caserta, M., Triassi, M., & Pecchia, L. (2015). Acute mental stress assessment via short term HRV analysis in healthy adults: A systematic review with meta-analysis. *Biomedical Signal Processing and Control*, 18, 370-377.
15. Li, Q., Rajagopalan, C., & Clifford, G. D. (2014). A machine learning approach to multi-level ECG signal quality classification. *Computer methods and programs in biomedicine*, 117(3), 435-447.
16. Rizwan, M. F., Farhad, R., Mashuk, F., Islam, F., & Imam, M. H. (2019, January). Design of a biosignal based stress detection system using machine learning techniques. In 2019 international conference on robotics, electrical and signal processing techniques (ICREST) (pp. 364-368). IEEE.
17. Garg, P., Santhosh, J., Dengel, A., & Ishimaru, S. (2021, April). Stress detection by machine learning and wearable sensors. In 26th International Conference on Intelligent User Interfaces-Companion (pp. 43-45).
18. Bobade, P., & Vani, M. (2020, July). Stress detection with machine learning and deep learning using multimodal physiological data. In 2020 Second International Conference on Inventive Research in Computing Applications (ICIRCA) (pp. 51-57). IEEE.
19. Rosales, M. A., Bandala, A. A., Vicerra, R. R., & Dadios, E. P. (2019, November). Physiological-Based Smart Stress Detector using Machine Learning Algorithms. In 2019 IEEE 11th International Conference on Humanoid, Nanotechnology, Information Technology, Communication and Control, Environment, and Management (HNICEM) (pp. 1-6). IEEE.

20. Ahuja, R., & Banga, A. (2019). Mental stress detection in university students using machine learning algorithms. *Procedia Computer Science*, 152, 349-353.
21. García-González, M. A., Argelagós-Palau, A., Fernández-Chimeno, M., & Ramos-Castro, J. (2013, September). A comparison of heartbeat detectors for the seismocardiogram. In *Computing in Cardiology 2013* (pp. 461-464). IEEE.
22. Goldberger, A. L., Amaral, L. A., Glass, L., Hausdorff, J. M., Ivanov, P. C., Mark, R. G., ... & Stanley, H. E. (2000). PhysioBank, PhysioToolkit, and PhysioNet: components of a new research resource for complex physiologic signals. *circulation*, 101(23), e215-e220.
23. Por, E., van Kooten, M., & Sarkovic, V. (2019). Nyquist–Shannon sampling theorem. *Leiden University*, 1(1).
24. SciPy. (2023). `scipy.signal.resample`.
25. Heckbert, P. (1995). Fourier transforms and the fast Fourier transform (FFT) algorithm. *Computer Graphics*, 2(1995), 15-463.
26. SciPy. (2023). `scipy.signal.resample`.
27. Shouran, M., & Elgamli, E. (2020). Design and implementation of Butterworth filter. *Mokhtar Shouran, Elmazeg Elgamli-International Journal of Innovative Research in Science, Engineering and Technology*, 9(9).
28. Fedotov, A. A. (2016). Selection of parameters of bandpass filtering of the ECG signal for heart rhythm monitoring systems. *Bio-medical Engineering*, 50, 114-118.
29. Neurokit. (2023). `Ecg`.
30. Chen, D., Wan, S., Xiang, J., & Bao, F. S. (2017). A high-performance seizure detection algorithm based on Discrete Wavelet Transform (DWT) and EEG. *PloS one*, 12(3), e0173138.
31. Neurokit, “Hrv,” accessed: August 27, 2023.
32. Jwo, D. J., Chang, W. Y., & Wu, I. H. (2021). Windowing techniques, the welch method for improvement of power spectrum estimation. *Comput. Mater. Contin.*, 67, 3983-4003.
33. Pandas, “`pandas.dataframe.corr`,” accessed: August 27, 2023.
34. Mukaka, M. M. (2012). A guide to appropriate use of correlation coefficient in medical research. *Malawi medical journal*, 24(3), 69-71.
35. Gómez-Chova, L., Calpe, J., Camps-Valls, G., Martín, J. D., Soria, E., Vila, J., ... & Moreno, J. (2003, July). Feature selection of hyperspectral data through local correlation and SFFS for crop classification. In *IGARSS 2003. 2003 IEEE International Geoscience and Remote Sensing Symposium. Proceedings (IEEE Cat. No. 03CH37477)* (Vol. 1, pp. 555-557). IEEE.
36. Guyon, I. (2008). Practical feature selection: from correlation to causality. *Mining massive data sets for security: advances in data mining, search, social networks and text mining, and their applications to security*, 27-43.
37. Pandas. (2023). “`pandas.dataframe.boxplot`,”
38. Abdi, H., & Williams, L. J. (2010). Principal component analysis. *Wiley interdisciplinary reviews: computational statistics*, 2(4), 433-459.
39. Maulud, D., & Abdulazeez, A. M. (2020). A review on linear regression comprehensive in machine learning. *Journal of Applied Science and Technology Trends*, 1(4), 140-147.
40. Zhang, Z. (2016). Introduction to machine learning: k-nearest neighbors. *Annals of translational medicine*, 4(11).
41. Lawrence, R. L., & Wright, A. (2001). Rule-based classification systems using classification and regression tree (CART) analysis. *Photogrammetric engineering and remote sensing*, 67(10), 1137-1142.
42. Berrar, D. (2018). Bayes’ theorem and naive Bayes classifier. *Encyclopedia of bioinformatics and computational biology: ABC of bioinformatics*, 403, 412.
43. Noble, W. S. (2006). What is a support vector machine?. *Nature biotechnology*, 24(12), 1565-1567.
44. Chen, T., He, T., Benesty, M., Khotilovich, V., Tang, Y., Cho, H., ... & Zhou, T. (2015). Xgboost: extreme gradient boosting. *R package version 0.4-2*, 1(4), 1-4.
45. Xanthopoulos, P., Pardalos, P. M., Trafalis, T. B., Xanthopoulos, P., Pardalos, P. M., & Trafalis, T. B. (2013). Linear discriminant analysis. *Robust data mining*, 27-33.
46. Dietterich, T. (1995). Overfitting and undercomputing in machine learning. *ACM computing surveys (CSUR)*, 27(3), 326-327.
47. Hannun, A., Guo, C., & van der Maaten, L. (2021, December). Measuring data leakage in machine-learning models with Fisher information. In *Uncertainty in Artificial Intelligence* (pp. 760-770). PMLR.
48. Berrar, D. (2019). Cross-Validation.
49. Hicks, S. A., Strümke, I., Thambawita, V., Hammou, M., Riegler, M. A., Halvorsen, P., & Parasa, S. (2022). On evaluation metrics for medical applications of artificial intelligence. *Scientific reports*, 12(1), 5979.

Copyright: ©2023 Dhrithi Rachepalli. This is an open-access article distributed under the terms of the Creative Commons Attribution License, which permits unrestricted use, distribution, and reproduction in any medium, provided the original author and source are credited.